Electroabsorption spectroscopy of molecular inorganic compounds

Fredrick W. Vance; Robert D. Williams; Joseph T. Hupp

PLEASE SCROLL DOWN FOR ARTICLE

Electroabsorption spectroscopy of molecular inorganic compounds

by FREDRICK W. VANCE, ROBERT D. WILLIAMS and JOSEPH T. HUPP

Department of Chemistry and Materials Research Center, Northwestern University, Evanston, IL 60208, USA

Electroabsorption spectroscopy is known to report directly on the changes in dipole moment and molecular polarizability accompanying electronic excited state formation. Because ground-state/excited-state dipole moment changes can be equated with effective one-electron transfer distances, experimental electroabsorption spectroscopy holds exceptional promise as a methodology for investigating light-induced charge transfer processes within inorganic systems. A survey of the available studies, including metal-to-ligand charge transfer, ligand-to-metal charge transfer and localized and delocalized 'intervalence' charge transfer studies, is presented. Also surveyed are electroabsorption studies aimed at illuminating selected molecular nonlinear optical responses. A general observation from electroabsorption studies has been that experimentally determined one-electron transfer distances are less than simple geometric descriptions would predict. Mononuclear transition-metal systems have proven to be good models for unravelling the complicating effects of ground-state localization and many-electron polarization. The capability of electroabsorption spectroscopy to resolve fundamental questions relating to electronic localization and delocalization has been highlighted in a series of studies in bridged dinuclear and tris(diimine) systems. The available electroabsorption data have also been used to reassess a number of molecular charge-transfer related parameters such as the electronic coupling energies and solvent reorganization energies. Very recent studies of putative octupolar complexes and donor–acceptor porphyrinic structures have highlighted the utility of electroabsorption spectroscopy for evaluating second-order nonlinear optical response mechanisms and for providing detailed information about state-specific contributions to overall molecular hyperpolarizabilities.

1.   Introduction

Johannes Stark's discovery of the splitting of spectral lines of atoms in the presence of an applied electric field, an achievement rewarded with the 1919 Nobel Prize in physics, marked the beginning of a new type of spectroscopy. Unfortunately, even though discussions of the Stark effect can be found in most physical chemistry textbooks [1], it was not until the 1970s that applications of Stark spectroscopy had moved from studies by physicists of atoms and simple molecules to studies of chemically [2] and biologically [3] interesting systems. In fact, only in the last ten years has the field been rediscovered *en masse*, spurred largely by the pioneering work of Boxer and co-workers [4, 5]. Why the renaissance in Stark spectroscopy?

Chemists have long been interested in probing the excited states of molecules. Of particular interest has been quantitatively determining many of the physical parameters associated with the transfer of charge. Stark spectroscopy is a straightforward, relatively unambiguous way to determine several of these parameters. When a disordered, immobilized sample is subjected to a large electric field, the absorption spectrum is perturbed by the field–molecule interaction ('electroabsorption spectroscopy'), and it has been shown that these perturbations can be directly related to

changes in the system's dipole moment ($\Delta\mu$), polarizability ($\Delta\alpha$), and transition moment.

Most studies to date have focused on elucidating the $\Delta\mu$ contribution to the Stark signal. Since $\Delta\mu$ can be interpreted as the product of charge and the distance through which charge is transferred, these studies have settled some long-standing debates over questions pertaining to charge localization/delocalization. More recent work is focusing on the relationship between $\Delta\mu$ and nonlinear optical parameters [6, 7] since theoretical models have indicated that $\Delta\mu$ should be directly correlated with the first hyperpolarizability, β.

Although changes in the transition moment and polarizability ($\Delta\alpha$) have not been studied as extensively as dipole moment changes, recent work is beginning to indicate that these parameters may also contribute significantly to our understanding of charge transfer and related processes.

Since several reviews of Stark spectroscopic methods as they pertain to biological [8] and materials systems [9] have recently appeared, we will focus exclusively on applications involving inorganic complexes. We will take a case study approach since any particular case illustrates a number of effects related to the molecular parameters under study.

2.   Background

The resurgence of interest in electroabsorption spectroscopy has doubtless been driven by elegant theoretical interpretations originating with Liptay [10] and extended by others [11]. As the details of the theoretical approach depend strongly on the sample and experimental conditions, we will follow the lead of Reimers and Hush who have applied the theory to inorganic compounds immobilized in glasses [12].

The sample is assumed to be completely isotropic, with an absorption band, $A(\nu)$, arising from a single molecular electronic transition†. When an external electric field, $\mathbf{F}_{\text{ext}}$, is applied to the sample, the field experienced by each molecule, $\mathbf{F}_{\text{int}}$, is given by:
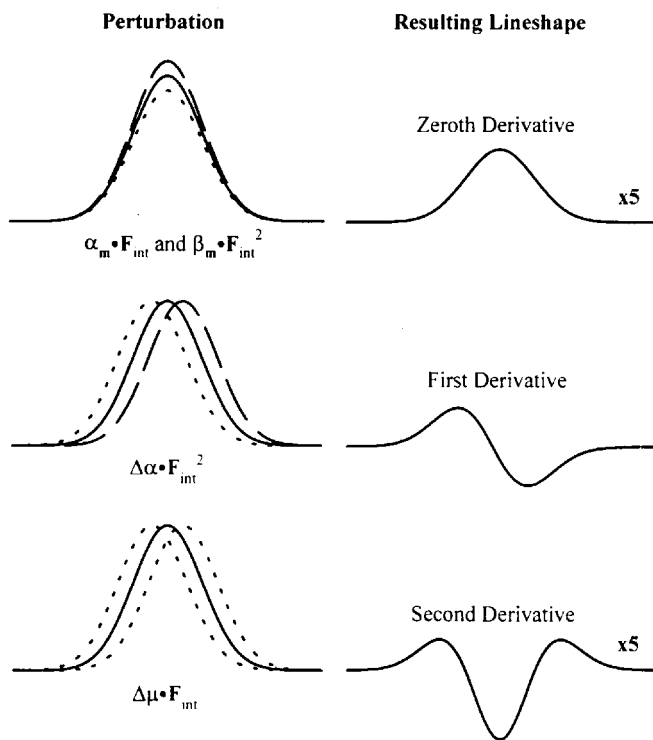
$$\mathbf{F}_{\text{int}} = f\mathbf{F}_{\text{ext}}. \tag{1}$$

Here f is the local field correction, generally believed to lie between 1 and 1.3 for glassed solvents, and the boldface type signifies a vector (or tensor) quantity. If the molecule is considered to reside in a dielectric medium forming a spherical solvation cavity, then the correction factor can be calculated from equation (2) [13]:

$$f = \frac{3D_s}{2D_s + 1}. \tag{2}$$

Here D_s is the static dielectric constant for the medium, a value which generally must be independently established or estimated for glassed solvents. Measuring the capacitance of the experimental glass and comparing it with that for solvents with known dielectric constants has proved useful for assessing D_s. For example, in one

---

† Among other assumptions made are: (a) that the electro-optic parameters are the same for all sublevels of the electronic transition (breakdown of this approximation has been addressed: Wortmann, R., Karsten, E., and Liptay, W., 1988, *Chem. Phys.*, **124**, 395), and (b) that the shape of the electronic transition does not change. In addition, for our purposes we will discuss only the electroabsorption of immobilized samples, so that migration and/or orientation of the sample in the field is not a possibility.

Perturbation	Resulting Lineshape

$\alpha_m \cdot F_{int}$ and $\beta_m \cdot F_{int}^2$ — Zeroth Derivative — x5

$\Delta\alpha \cdot F_{int}^2$ — First Derivative

$\Delta\mu \cdot F_{int}$ — Second Derivative — x5

Scheme 1

study using water/ethylene glycol as the solvent matrix, D_s was determined to be ~ 3.7, resulting in an estimated local field correction factor of $f \approx 1.3$ [14]†.

The local field may perturb the absorbance spectrum in several ways. Modification of the transition moment vector **m** represents one perturbation‡, and changes in the energies of the initial and final states represent a second. Changes in **m** are manifested as uniform increases or decreases in the extinction coefficient of the transition. Therefore, they yield difference spectra that are shaped much like the unperturbed absorption spectrum (see scheme 1). Equation (3) summarizes the expected field dependence of **m**:

$$m(F_{int}) = m + \alpha_m \cdot F_{int} + F_{int} \cdot \beta_m \cdot F_{int} \qquad (3)$$

In the equation, α_m and β_m are the transition moment polarizability and hyper-polarizability tensors, respectively. While the β_m term is generally considered to be negligible at the field strengths used experimentally, the α_m term also is typically small. Exceptions are expected when imposition of an electric field significantly alters the degree of applicability of a particular selection rule or rules. As seen in scheme 1, differential changes in initial and final state energies with an applied electric field are manifest experimentally as changes in E_{op}, the energy maximum of the absorption

---

† Recent work (Bublitz, G. U., and Boxer, S. G., 1997, private communication) has suggested that f values may be systematically underestimated by continuum models since the local polarity around a solute typically increases upon freezing.

‡ The transition moment vector has also been denoted μ_{eg} in other bodies of work, but is denoted **m** here to distinguish it from the state dipole moment vectors.
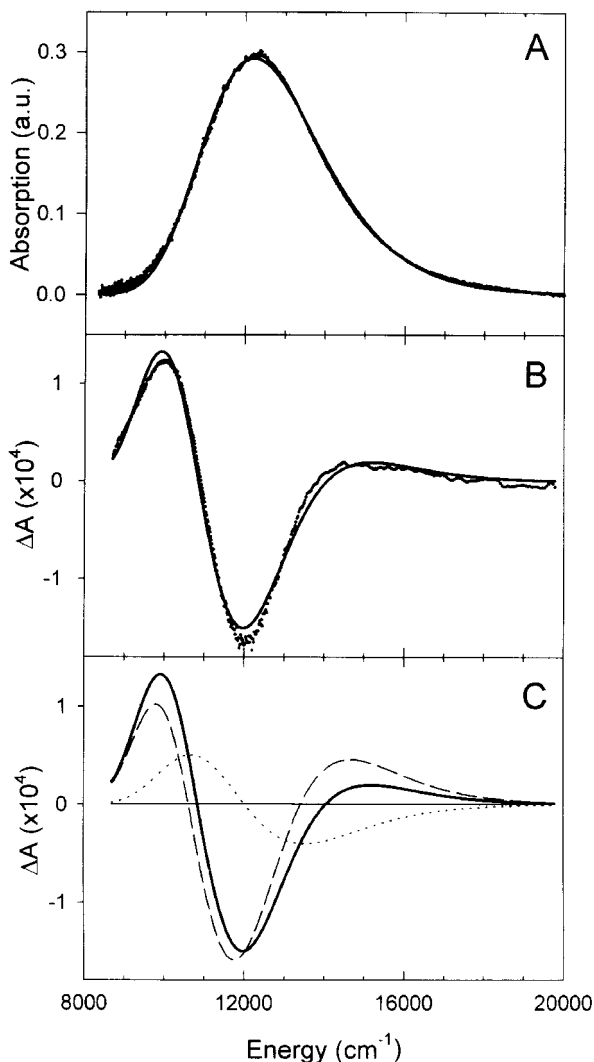
Figure 1. Electroabsorption (*a*) 77 K absorption spectrum with fit to gaussian curve. (*b*) Electroabsorption spectra ($\chi = 54.7°$) with fit to equation (5). (*c*) Fit to equation (5) (thick solid line) along with zeroth (solid, thin), first (dotted), and second (dashed) derivative contributions.

spectrum. As indicated in equation (4), energy shifts are further related to the changes in dipole moment ($\Delta\mu$) and polarizability ($\Delta\alpha$) accompanying ground-state to excited-state conversion.

$$\Delta E_{op}(\mathbf{F}_{int}) = E_{op}(\mathbf{F}_{int}) - E_{op}(0) = -\Delta\mu \cdot \mathbf{F}_{int} - \tfrac{1}{2}\mathbf{F}_{int} \cdot \Delta\alpha \cdot \mathbf{F}_{int}. \qquad (4)$$

Qualitatively, the appearance in the electroabsorption spectrum of the two terms in equation (4) may be understood fairly straightforwardly. For the first term ($-\Delta\mu \cdot \mathbf{F}_{int}$), suppose that the molecular possesses a larger dipole moment in the excited state than in the ground state (i.e. $\Delta\mu > 0$). Those molecular dipoles (chromophores) that are aligned with the applied field will suffer a decrease in the optical charge transfer transition energy, while those aligned against the field will

experience an increase. Since the molecules (and dipoles) are randomly oriented in the sample, the overall effect will be a broadening of the transition so that the difference spectrum will resemble the second derivative of the unperturbed spectrum. (In the opposite case, where the ground state dipole moment is larger than the excited state, the effect of the applied field on the respective states is reversed, but the resulting difference spectrum will be the same.) For the second term ($-\frac{1}{2}\mathbf{F}_{int} \cdot \Delta\boldsymbol{\alpha} \cdot \mathbf{F}_{int}$), imagine the applied field inducing its own dipole moment in a polarizable sample (regardless of any permanent dipoles). This time, since the dipoles are field-induced they will all be aligned in the same direction and the transition energy will shift in only one direction—thereby yielding a difference spectrum ('Stark spectrum') resembling the first derivative of the unperturbed spectrum.

Hence, the perturbations in equation (3) and (4) can be used to describe the overall change in the absorption spectrum, $\Delta A(\nu)$, as a linear combination of the zeroth, first, and second derivatives of the absorption spectrum, $A(\nu)$ [6(a)]:

$$\Delta A(\nu) = \left\{ A_\chi A(\nu) + \frac{B_\chi \nu}{15hc}\frac{d[A(\nu)/\nu]}{d\nu} + \frac{C_\chi \nu}{30h^2c^2}\frac{d^2[A(\nu)/\nu]}{d\nu^2} \right\} \mathbf{F}_{int}^2, \qquad (5)$$

where the resulting coefficients A_χ, B_χ, and C_χ generally provide information about the changes in the transition moment, polarizability, and dipole moment respectively (see figure 1 and table 1).

For polarized light striking the sample at an angle χ with respect to the electric field, the zeroth derivative coefficient A_χ is described by [6(a)]:

$$A_\chi = \frac{1}{30|\mathbf{m}|^2}\sum_{ij}[\alpha_{ij}^2 + (3\cos^2\chi - 1)(3\alpha_{ii}\,\alpha_{jj} + 3\alpha_{ij}\alpha_j + 2\alpha_{ij}^2)] \qquad (6a)$$

$$+ \frac{1}{15|\mathbf{m}|^2}\sum_{ij}[10m_i\,\beta_{ijj} + (3\cos^2\chi - 1)(3m_i\,\beta_{jij} + 3m_i\,\beta_{jji} - 2m_i\,\beta_{ijj})].$$

In equation (6a), the subscripts i and j refer to components of the vectors or tensors and the summation is carried out over the spatial coordinates x, y, and z. Note that A_χ depends only on the transition moment polarizability and hyperpolarizability tensors (cf. equation (3)). At the magic angle of $\chi = 54.7°$ equation (6a) reduces to (6b):

$$A_\chi = \frac{1}{30|\mathbf{m}|^2}\sum_{ij}\alpha_{ij}^2 + \frac{1}{15|\mathbf{m}|^2}\sum_{ij}10m_i\,\beta_{ijj}. \qquad (6b)$$

In a similar manner, the coefficient for the first derivative component, B_χ, is described by equation (7a), where $\mathrm{Tr}(\Delta\boldsymbol{\alpha})$ is the trace of the change in polarizability [6(a)]:

$$B_\chi = \frac{5}{2}\mathrm{Tr}(\Delta\boldsymbol{\alpha}) + (3\cos^2\chi - 1)\left(\frac{3}{2}\frac{\mathbf{m}\cdot\Delta\boldsymbol{\alpha}\cdot\mathbf{m}}{|\mathbf{m}|^2} - \frac{1}{2}\mathrm{Tr}(\Delta\boldsymbol{\alpha})\right) \qquad (7a)$$

$$+ \frac{1}{|\mathbf{m}|^2}\sum_{ij}[10m_i\,\alpha_{ij}\,\Delta\mu_j + (3\cos^2\chi - 1)(3m_i\,\alpha_j\,\Delta\mu_j + 3m_i\,\alpha_{jj}\Delta\mu_i - 2m_i\,\alpha_{ij}\,\Delta\mu_j)].$$

It can be seen that the B_χ coefficient depends strongly on the change in polarizability, $\Delta\boldsymbol{\alpha}$. Rewriting equation (7a) for the case where $\chi = 54.7°$ yields:

$$B_\chi = \frac{5}{2}\mathrm{Tr}(\Delta\boldsymbol{\alpha}) + \frac{1}{|\mathbf{m}|^2}\sum_{ij}10m_i\,\alpha_{ij}\,\Delta\mu_j. \qquad (7b)$$

Table 1. Summary of quantities involved in electroabsorption experiment.

Coefficient	Derivative	Information acquired	Implications/Applications
A_χ	Zeroth	α_m and β_m	forbidden/allowed transitions
B_χ	First	$Tr(\Delta\alpha)$ and $\alpha \cdot \Delta\mu$	polarizability ($\Delta\alpha$) excited state description
C_χ	Second	$\Delta\mu$ and ζ	charge transfer distance ($\Delta\mu$) electronic coupling ($\Delta\mu$) solvent reorganization ($\Delta\mu$) charge transfer symmetry (ζ) 2nd order NLO response ($\Delta\mu$)

The second term of equation (7*b*) shows that the coefficient is also dependent on a product term involving the transition moment polarizability tensor, α_m, and the change in dipole moment, $\Delta\mu$. Since it is typically difficult or impossible to separate the $\Delta\alpha$ term from the product term experimentally, an assumption is usually made that one of the two components of equation (7*b*) goes to zero. In many of the case studies described below, the $Tr(\Delta\alpha)$ term has been regarded as dominant and the product term has been neglected. Shin *et al.* [7] have suggested, however, that under some conditions the product term can be significant and furthermore, that its magnitude can be suitably estimated via a two-level model. For a one-dimensional case (i.e. polarizability alteration and charge transfer exclusively along the light absorption (transition dipole moment) axis), the B_χ expression (two-level model) becomes:

$$B_\chi = \frac{5}{2} Tr(\Delta\alpha) + \frac{10(\Delta\mu)^2}{E_{op}(0)}. \tag{7c}$$

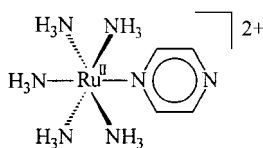Finally, the second derivative component is represented by the coefficient C_χ in equation (8)

$$C_\chi = |\Delta\mu|^2 [5 + (3\cos^2\chi - 1)(3\cos^2\zeta - 1)]. \tag{8}$$

The direct dependence on $\Delta\mu$ makes this coefficient the most straightforward to interpret, especially when $\chi = 54.7°$. At other angles it is possible to interrogate ζ, the angle between **m** and $\Delta\mu$. For simple linear charge transfer systems in one dimension, ζ is expected to be zero, an expectation frequently borne out by experimental results. For systems for which ζ is zero, therefore, the vector and tensor quantities can usually be written (without boldface) as one dimensional scalar quantities, e.g. $\Delta\mu$.

3. Case studies
3.1. *MLCT and LMCT within Ru(NH$_3$)$_5$L$^{2+, 3+}$ complexes*

The intense, visible region metal-to-ligand charge transfer (MLCT) and ligand-to-metal charge transfer (LMCT) transitions found in amine complexes of Ru^{II} and Ru^{III}, respectively, have been the object of scrutiny for many years [15]. Oh and Boxer showed that the electroabsorption response of the MLCT region of Ru(NH$_3$)$_5$pyz^{2+} (shown below)

is dominated by a second derivative component, indicative of a large degree of charge transfer [4]. Complicating this, however, the presence of a low-energy feature in the electroabsorption spectrum indicated the existence of another electronic transition distinct from the main MLCT with, presumably, different electro-optic properties. In further work, they found that protonation of the pyrazine ligand in this complex yielded an electroabsorption spectrum dominated by zeroth and first derivative terms, instead of the second derivative term. By contrast, studies of $Ru(NH_3)_5(4,4^\prime$-bipyridine)$^{2+}$ revealed a second derivative lineshape in the unprotonated form, with an even greater degree of charge transfer upon protonation [4]. The effective (adiabatic) charge transfer distance, R_{12}, can be found from Stark spectroscopy by equation (9), where e is the unit charge:

$$\Delta\mu_{12} = e\,R_{12}. \tag{9}$$

Interestingly, for these systems the Stark-derived $\Delta\mu$'s result in R_{12}'s which are considerably smaller than the geometric separation of the metal and ligand centres.

Reimers and Hush, in theoretical papers based on Oh and Boxer's results, described how diminution of $\Delta\mu$—and by inference R_{12}—can arise from a combination of: (1) ground-state π back-bonding between dπ orbitals and the ligand LUMO, and (2) interaction of the perturbing field with the NH_3 ligands, leading to induced ligand dipole moments which partially cancel the metal–ligand dipole moment [12]. Their Liptay-based treatment of the electroabsorption phenomenon, combined with electronic structure calculations, showed that the Stark results were consistent with already existing electronic structure models for the two compounds and their protonated congeners [16].

More recently, Shin *et al.* have reported on a large number of compounds of the $Ru(NH_3)_5L^{2+,3+}$ form [7, 17] where L is an aromatic nitrogen-containing heterocycle or nitrile. Electroabsorption studies of metal-to-ligand charge transfer within the 2+ forms showed that the experimental $\Delta\mu$'s were, as in the Oh and Boxer systems, smaller than naive geometric arguments would predict, ranging from 4 to 23 D. (Note that 4.8 D is equivalent to 1 $e\text{Å}$.) They also tested the effects of changes in counter ion, concentration, and ionic strength of the samples, and found that the electroabsorption spectra were largely unperturbed. Studies of the LMCTs of the 3+ forms generally resulted in much greater $\Delta\mu$'s (16 to 37 D) than in MLCTs of the 2+ analogues.

$$(NH_3)_5Ru^{III}\!\!-\!N$$
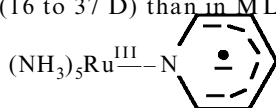
$$e \cdot R(\text{geometric}) = 12\ \text{D} = 2.5\ e\text{Å}$$

$$e \cdot R_{12} = 4\ \text{D} = 0.8\ e\text{Å}$$

As part of their explanation of these results, they agreed that the π back-bonding and ligand polarization effects invoked by Reimers and Hush [12] contributed to the measured responses. However, they emphasized that when charge is transferred from the metal to the ligand, the metal's higher charge causes the electron distribution in the ligand to shift toward the metal, opposing the dipole moment generated by the transferring charge. To support their hypothesis, Shin *et al.* utilized an INDO-SCF

based model which included not only the single electron transfer, but also accounted for the redistribution of the other electrons within the system [7, 17]. Computational studies by Zeng *et al.* have further explored this effect via *ab initio* and INDO based techniques and have yielded relatively good agreement between theory and experiment [18].

3.1.1. *Implications*

To better describe charge transfer processes, it is useful to calculate the charge transfer distance in the diabatic limit, R_{ab}. (In this context, 'diabatic' refers to the hypothetical or idealized condition of zero electronic interaction between the ground state and the charge transfer excited state. 'Adiabatic', on the other hand, refers to the condition where such interactions, and the resulting perturbations, are taken into account. Following Cave and Newton [19] we will denote diabatic quantities with subscript letters and adiabatic quantities with subscript numbers.) In the two-state limit, the diabatic charge transfer distance, R_{ab}, can be directly related to the *adiabatic* change in dipole moment, $\Delta\mu_{12}$ via [19]:

$$\Delta\mu_{ab} = e\,R_{ab} = [(\Delta\mu_{12})^2 + 4\mu_{12}^2]^{1/2}. \tag{10}$$

Here μ_{12} is the transition moment† for the transition of interest; it can be obtained from an absorption experiment by utilizing the relation [20]:

$$\mu_{12} = 2.06 \times 10^{-2} \left(\frac{\varepsilon_{max}\,\Delta\nu_{1/2}}{\nu_{max}\,b} \right)^{1/2}, \tag{11}$$

where ε_{max} is the molar extinction coefficient, $\Delta\nu_{1/2}$ is the electronic absorption full width at half maximum, ν_{max} is the energy of the absorbance maximum and b is a degeneracy term usually taken to be unity. For the MLCT transitions examined in the Shin study, the R_{ab}'s were considerably larger than the R_{12}'s, whereas for the LMCT transitions, the R_{ab} values were only marginally greater than the R_{12}'s.

Another way to describe charge-transfer systems is by the application of first order perturbation theory within a two-state model. In this approach, modelled on the early work of Mulliken [21] and Hush [22], the initial and final states for charge transfer (Ψ_1 and Ψ_2) are described as linear combinations of the zeroth-order (fully localized) states, Ψ_a and Ψ_b:

$$\Psi_1 = c_a\,\Psi_a + c_b\,\Psi_b, \tag{12}$$

$$\Psi_2 = c_a\,\Psi_a - c_b\,\Psi_b. \tag{13}$$

The coefficients c_a and c_b can be normalized by application of equation (14), where S_{ab} denotes the overlap between the orbitals a and b:

$$c_a^2 + c_b^2 \pm 2c_a\,c_b\,S_{ab} = 1. \tag{14}$$

If the overlap is small ($S_{ab} \ll 1$) then the squares of the coefficients themselves describe the fraction of the transferring electronic charge initially present at each site. A c_b^2 value of zero then indicates complete ground state valence localization at the donor site, while a c_b^2 of 0.5 indicates complete charge *de*localization between putative electron donor and acceptor sites. Finally, the amount of charge actually transferred between donor and acceptor sites as a consequence of optical excitation (e.g. LMCT, MLCT or other excitation) is $(1-2c_b^2)e$, where e is the unit electronic charge.

---

† Note that μ_{12} is equivalent to **m** in the preceeding section (see footnote on p. 309).

The important realization made by Shin *et al.* [7] was that the delocalization parameter c_b^2 could be directly related to parameters obtained from Stark spectroscopy via:

$$c_b^2 = \frac{1}{2}\left[1 - \left(\frac{\Delta\mu_{12}^2}{\Delta\mu_{12}^2 + 4\mu_{12}^2}\right)^{1/2}\right] = \frac{1}{2}\left[1 - \frac{\Delta\mu_{12}}{\Delta\mu_{ab}}\right]. \tag{15}$$

Applying this description to the transitions studied showed that while LMCT transitions to Ru^{III} could generally be described as occurring between predominantly charge localized ground and excited states ($0.005 \leqslant c_b^2 \leqslant 0.02$; $0.98 \leqslant c_a^2 \leqslant 0.995$), the MLCT transitions from Ru^{II} involved states which were significantly more delocalized; ($0.02 \leqslant c_b^2 \leqslant 0.5$; $0.5 \leqslant c_a^2 \leqslant 0.98$). In part, the differences reflect the typically greater energy gaps associated with the LMCT transitions in comparison to MLCT transitions (cf. equations (10), (11) and (15)).

3.2. $(NH_3)_5Ru\text{-}4,4'\text{-}bipyridine\text{-}Ru(NH_3)_3^{n+}$: valence localization and thermal electron transfer

This molecule, with three accessible charge states (overall $4+$, $5+$, or $6+$), has been extensively characterized by a variety of techniques and represents one of the early successes of Hush's theoretical description of mixed-valence dimers [22(*a*), 23]. Intense transitions assigned to metal-to-ligand charge transfer (MLCT) characterize the visible region absorption spectrum of both the fully reduced ($4+$) and the mixed-valence ($5+$) forms [24]. The latter form has an additional transition in the near-infrared which has been assigned to intervalence charge transfer (IVCT) as shown below:

$$\tag{16}$$
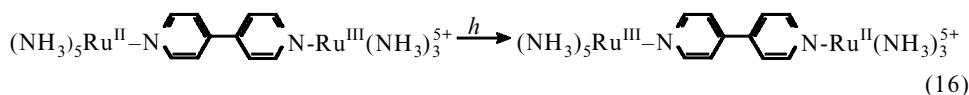
Application of Hush theory to its intensity, width and energy maximum yielded the conclusion that the mixed-valence state is almost completely valence localized (i.e. $Ru^{2.02}\text{-}L\text{-}Ru^{2.98}$). Although the Hush description was largely consistent with other experimental observations, a few problems remained. One was the considerable discrepancy between the experimental and theoretical values for the solvent re-organization energy (λ_s).

The electroabsorption responses of both the MLCT and IVCT transitions of this compound were measured by Oh and Boxer, with the former transition also examined as a function of the overall charge [4]. For both the $4+$ and $5+$ forms, the visible region MLCT spectrum was complicated by the presence of overlapping transitions that could not easily be deconvoluted. The IVCT transition in the near-infrared region was found, however, to be dominated by the second derivative of the absorbance, from which a $|\Delta\mu|$ value of *ca.* 21 D was extracted. In this case, although 21 D ($= 4.4\ e\text{Å}$) clearly substantiates the trapped valence description, it represents only about 40% of the value expected based on full charge transfer over the entire metal–metal separation distance.

As pointed out by Hupp and co-workers [25], diminution of the effective charge transfer distance has interesting ramifications in terms of several Hush-related parameters. Theoretical values for λ_s may be calculated by using various dielectric continuum models in which λ_s is directly related to the charge transfer distance (cf.
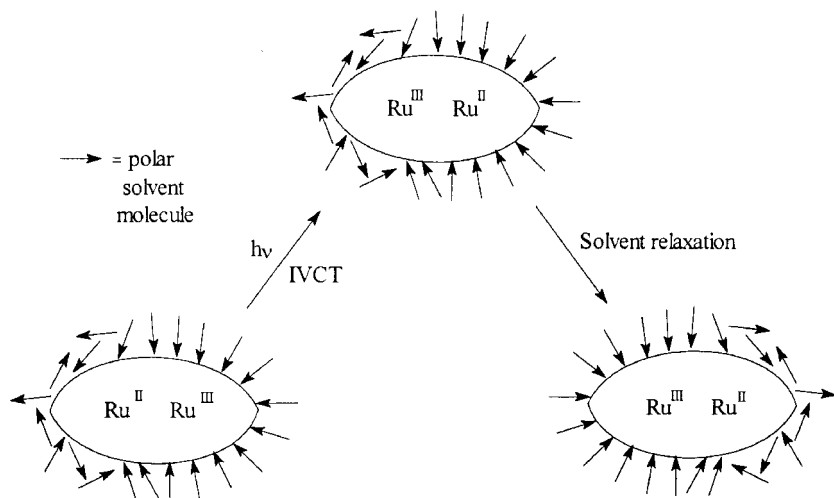
Scheme 2

scheme 2) [26]. Since Oh and Boxer's results imply a much diminished R_{ab} value, they ultimately yield much smaller continuum values for λ_s. The new values are, in fact, in excellent agreement with the experimentally determined λ_s values.

Limiting expressions for the electronic coupling parameter H_{ab} are also intimately related to $\Delta\mu_{ab}$, in this case by [19]:

$$H_{ab} = \frac{\mu_{12}\ \nu_{max}}{\Delta\mu_{ab}} \tag{17}$$

Previous estimates for H_{ab}, obtained by using the geometric metal–metal separation distance for R_{ab}, were *ca.* 460 cm^{-1} in water as solvent; use of the revised R_{ab} value increased the H_{ab} estimate to 1020 cm^{-1} [25]. This revision has particular significance for the thermal electron transfer rate (see figure 2 and equation (18)) since, at least for weakly electronically coupled systems, the rate is proportional to the square of H_{ab} [27].
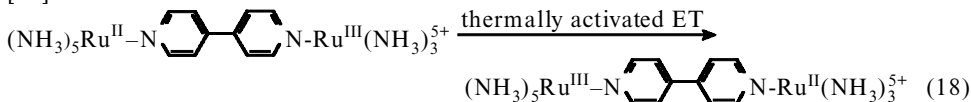
Thus, the revision suggests a *ca.* 5-fold increase in the estimated rate of (thermal) intramolecular electron transfer. Also expected to enhance the rate is a 'barrier rounding' effect (diminution of ΔG^*) caused by adiabatic surface splitting in the classical diabatic surface crossing region; see figure 2. Note that the magnitude of the barrier rounding effect, for a two-level system, will be precisely H_{ab}.

3.3. $(NH_3)_5Ru$-pyrazine-$Ru(NH_3)_5^{n+}$: valence delocalization

This compound, often referred to as the Creutz–Taube ion, is structurally similar to the 4,4′-bipyridine-bridged compound just discussed, but was actually prepared and studied first [23(b), 28]. Like its cousin, it has three accessible oxidation states, with both the 4+ and 5+ forms characterized by intense, visible region MLCT absorption, with a near-infrared 'IVCT' transition found in the mixed-valence species. Unlike its
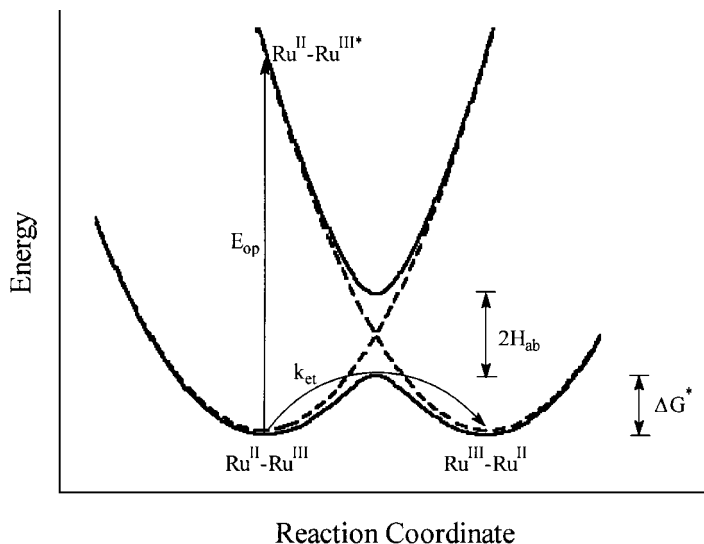
Figure 2. Potential energy surfaces for optical and thermal electron transfer in $(NH_3)_5Ru-$
4,4′−bpy−$Ru(NH_3)_5^{5+}$. Dashed line: diabatic surfaces. Solid line: adiabatic surfaces with
$H_{ab} = 1020$ cm^{-1}.

cousin, however, the relatively narrow and solvent independent IVCT has not been
amenable to a Hush interpretation. Instead, Piepho, Krausz and Schatz (PKS)
advanced a two-site vibronic coupling model [29] to explain the near-infrared
lineshape, which was later followed by a three-site molecular orbital picture proposed
by Ondrechen [30]. Extensions to the original PKS model have also been made [31].
Regardless of theory, the fundamental question has long been whether the odd
electron in the mixed-valence form is valence localized, as in the 4,4′-bipyridine
analogue, or is valence delocalized.

Oh and Boxer recognized that a negligible second derivative contribution to the
electroabsorption signal would be characteristic of valence delocalization, whereas
valence localization would give rise to a substantial second derivative contribution.
Their Stark results on the IVCT of the mixed-valence compound [4], which showed a
$|\Delta\mu|$ value of only *ca.* 0.5 D (as compared to the 33 D expected for unit charge transfer
over the full geometric distance), combined with a preponderance of evidence from
other experiments such as resonance Raman [32], infrared [33], magnetic circular
dichroism [34], and others [35] has led to the conclusion that the mixed-valence ion
is indeed valence delocalized.

Substitution of N-containing heterocycles in the position *trans* to the bridging
pyrazine may competitively disrupt the ruthenium dπ to pyrazine π^* back-bonding
and induce some degree of valence trapping.
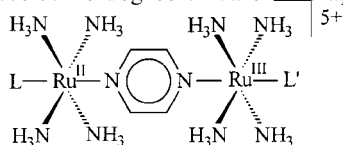
L = NH$_3$, 2,6-dimethylpyrazine, pyridine
L' = 2,6-dimethylpyrazine, pyridine

Several *trans*-substituted variants of the Creutz–Taube ion have been synthesized and
studied by Curtis and co-workers [36]. Interestingly, symmetric variants (i.e. same
trans ligand on each end of the molecule) appear to be largely valence delocalized,
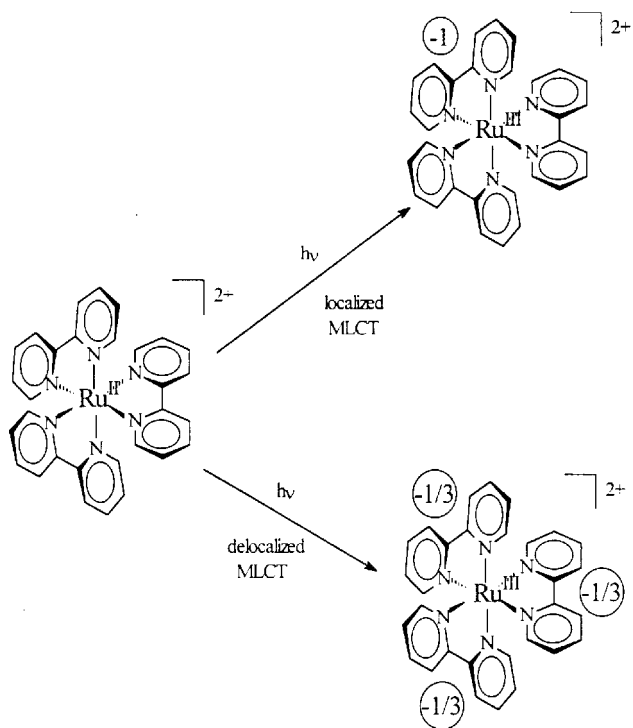
Scheme 3

while asymmetric variants (different *trans* ligands) bear some of the signatures of valence localization. Recent electroabsorption studies have revealed that the electro-absorption lineshape is fundamentally different for symmetric versus asymmetric derivatives [37]. For example, the Stark spectral lineshape of the pyridine-substituted symmetric derivative is reminiscent of the Creutz–Taube ion itself, while the lineshape of the asymmetric pyridine-substituted derivative is roughly the negative of that of the Creutz–Taube. These differences are believed to involve primarily changes in the zeroth (transition dipole) and first ($\Delta\alpha$) derivative terms† whose origin is apparently related to the unusual three-centre bonding scheme which has been used successfully to describe valence delocalized systems [30].

3.4. $Ru(2,2'-bipyridine)_3^{2+}$

The visible region of the absorbance spectrum of this compound consists of at least three overlapping MLCT transitions: two transitions to singlet states found at higher energy, and a transition to a triplet state found at lower energy [38]. Considerable debate had centred on the question of whether charge is localized on one of the bipyridine ligands or delocalized over all three (scheme 3). Although compelling evidence for excited-state charge localization had already been found by transient resonance Raman [39] and other techniques [40], the observation of a relatively large

---

† There appears to be relatively little second derivative character in the electroabsorption of any of the Creutz–Taube derivatives. Certainly valence localization even in the asym-metrically substituted 2,6-dimethylpyrazine derivative is—at best—only partial, not resembling the strongly localized bridging 4,4′-bipyridine molecule (section 3.2).

$|\Delta\mu|$ via electroabsorption spectroscopy would again be definitive. Furthermore, in contrast to the Raman experiments, the Stark measurement would report on the *initially* formed excited state.

Electroabsorption results of Oh and Boxer [4(c), 5] indicated that absorption into the dominant singlet MLCT at 454 nm is coupled to a $|\Delta\mu|$ of *ca.* 7 D, corresponding to transfer of charge over *ca.* 50% of the geometric donor (metal)/ligand (acceptor) separation distance. Excitation into the next singlet state at 420 was also found to be accompanied by a large $|\Delta\mu|$, although it was less than the previous transition. Excitation into the triplet state (found as a shoulder in the absorbance band) was coupled to a slightly greater $|\Delta\mu|$. Interestingly, if the ground state has true D_3 symmetry, these $|\Delta\mu|$'s would also correspond directly to values for μ(excited state), since the ground state dipole moment would necessarily be zero. More recently, Hug and Boxer reported an electroabsorption study on the ultraviolet ligand-centred transitions in $M(bpy)_3^{2+}$ where M is Fe, Ru, Os or Zn. They found that the $|\Delta\mu|$'s associated with these transitions are, regardless of the identity of the metal, larger than would be expected if the transitions were purely ligand-centred [41]. They additionally found a correlation between the energy separation between the MLCT and the ligand-centred transition and the value of $|\Delta\mu|$. This, of course, would be consistent with energy-gap-controlled mixing of the MLCT and ligand-centred electronic excited states.

Oh has additionally studied the MLCT excitation of $Ru(bpy)_3^{2+}$ derivatives $Ru(bpy)_2(2,2'$-biquinoline$)^{2+}$ (shown below)
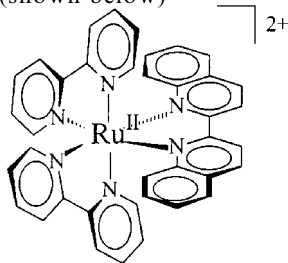
and $Ru(2,2'$-biquinoline$)_3^{2+}$ [4(c), 5]. The latter was found to display a slightly smaller $|\Delta\mu|$ than $Ru(bpy)_3^{2+}$. The mixed ligand complex, on the other hand, was of particular interest since charge transfer into each of the two ligand types can be distinguished in the absorption spectrum. Interestingly, $|\Delta\mu|$ for charge transfer to the bpy ligands within the mixed ligand complex was smaller than in $Ru(bpy)_3^{2+}$.

Although overlapping excitation to multiple states is often a problem in absorbance spectroscopy, emission usually occurs from only a single state. Hence, the problem of overlapping bands in the absorbance may potentially be alleviated by examining electro-emission rather than electroabsorption since, in principle, the Liptay treatment holds for either case [11(b)]. When electro-emission from these compounds was examined, however, it was found that the lineshapes were dominated not by second derivatives as was found in the absorbance case, but by negative zeroth derivatives. Only $Ru(bpy)_2($biquinoline$)^{2+}$ yielded an electro-emission response largely consistent with electroabsorption results. According to Oh [4(c)], electro-emission is likely complicated, however, by field tuning of decay mechanisms, field modulation of quantum yields, and possibly other effects.

### 3.5. *Ru(phenanthroline)$_3^{2+}$*

This compound (shown below),
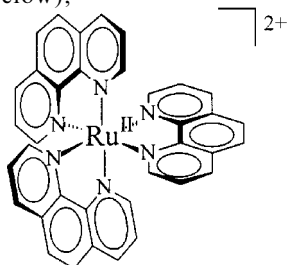
like $Ru(bpy)_3^{2+}$, is also characterized by overlapping visible region MLCTs [38]. Solvatochromic studies published concurrently with similar studies on $Ru(bpy)_3^{2+}$ indicated that charge is substantially localized on a single phenanthroline upon MLCT excitation [40]. There was, however, a contrary study in which transient resonance Raman spectroscopy indicated that charge was delocalized upon excitation, as evidenced by lack of the Raman signature for phenanthroline anion in the excited state [42].

In support of the solvatochromic work, electroabsorption spectroscopy by Karki and Hupp [43] demonstrated that excitation into the dominant, lowest energy singlet MLCT is accompanied by a $|\Delta\mu|$ of *ca.* 7 D, very close to the value reported for excitation into the dominant singlet of $Ru(bpy)_3^{2+}$ [5]. Interestingly, the electroabsorption spectrum of the triplet-forming transition was fairly strong, although its absorption spectrum was poorly resolved. The $|\Delta\mu|$ measured for this transition was 11 ± 4 D, again consistent with instantaneous formation of a localized excited state.

3.6. *Biruthenium tetraiminoethylenedimacrocycles: extreme delocalization*

This complex (shown below)
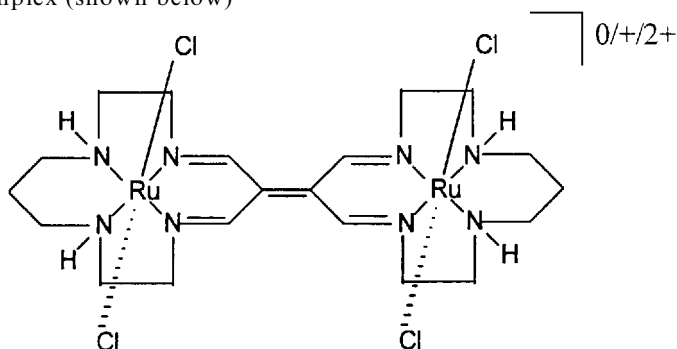
is part of a family of compounds prepared by Spreer and co-workers [44]. The reduced (Ru^{II},Ru^{II}) form is characterized by an intense low-energy transition ($\lambda_{max} = 910$ nm, $\varepsilon = 19\,000$ M^{-1} cm^{-1}) assigned to MLCT, while in the mixed-valence form there is an even more intense band found at 805 nm which has been assigned to 'IVCT'. Based on electrochemistry, X-ray photoelectron spectroscopy, and the solvent independence of the IVCT transition, it had been postulated that the odd electron in the mixed-valence form is strongly delocalized [44(*d*)].

Electroabsorption spectroscopy on this band has revealed that $|\Delta\mu|$ is on the order of 1 D, consistent with the delocalized description [45]. Interestingly, the spectroscopy

also revealed that the excited-state/ground-state polarizability difference ($Tr(\Delta\alpha)$) is small and negative. (Experimentally, $Tr(\Delta\alpha)$ values are usually positive.) This was attributed to a three-centre bonding mechanism hypothesized to be operative in delocalized mixed-valence systems in which the odd electron in the ground state is symmetrically delocalized over both metals and the bridging ligand whereas in the excited state it is found only on the metals [30]. This unusual bonding scheme may paradoxically lead to an excited state that is less polarizable than the ground state. An alternative explanation consistent with the data would involve decoupling of the IVCT excited state from higher lying states.

3.7. $(NC)_5Fe^{II}-CN-Os^{III}(NH_3)_5^{1-}$: asymmetric intervalence charge transfer

Since Stark spectroscopy provides a direct means to evaluate the one-electron transfer distance for optical transitions, it can provide information necessary to estimate ET reaction parameters such as the electronic coupling matrix element, H_{ab}, and the solvent reorganization energy, λ_s (cf. section 3.2). This capability has recently been applied to the optical intervalence charge transfer (IVCT) reaction occurring within $(NC)_5Fe^{II}-CN-Os^{III}(NH_3)_5^{1-}$ [46]. The electroabsorption spectrum in the intervalence region is dominated by a second derivative component, which readily yields the charge transfer distance, R_{12}, from equations (8) and (9). For this reaction, $eR_{12} = 2.5 \pm 0.3\ e\text{Å}$. By comparison, the geometric metal (donor)/metal (acceptor) separation distance is 5.0 Å [47]†. An obvious explanation for the discrepancy is that significant partial delocalization exists and the effective amount of charge transferred is much less that the unit electronic charge (e). (Recall that the effective amount of charge transferred is $(1-2c_b^2)e$.) To evaluate this possibility, the corresponding *non adiabatic* charge transfer distance, R_{ab}, was calculated from equation (10). The value obtained was 2.8 Å—still less than 60% of the geometric distance.

It should be noted that there is a small discrepancy between the nonadiabatic distance reported here and that in the original work [46]. The difference is due to the treatment of degeneracy in equation (11) for the transition moment, μ_{12}. In the original work, the transition was taken as doubly degenerate, to allow for both d_{xz} and d_{yz} transitions. However, for both transitions to occur with equal probability, the component octahedral coordination assemblies would need to be configured at 45° with respect to each other, along the z axis. (The z axis is defined as the metal–metal axis.) Recent X-ray crystallographic studies [47] have shown that the octahedra are nearly aligned, indicating that only one of the two putative donor orbitals can effectively participate. Thus, the correct degeneracy value is one, indicating a transition from *either* a d_{xz} or d_{yz} orbital.

The observation of an unusually small value for R_{ab} has significant implications in terms of the energetics of charge transfer. For example, the solvent reorganization energy, which can be modelled in a simple spherical or ellipsoidal cavity, is—to a very rough approximation—proportional to R_{ab}. The measured R_{ab} value leads to $\lambda_s = 2550\ \text{cm}^{-1}$, whereas a previous estimate, based on the geometric separation distance, suggested a value as high as $7000\ \text{cm}^{-1}$. Another important revision is the calculated value for the electronic coupling matrix element, H_{ab}. A nonadiabatic distance of 2.8 Å leads to $H_{ab} = 2460\ \text{cm}^{-1}$, which is smaller, by nearly a factor of two, than an estimate obtained based on electron transfer over the full metal–metal separation distance.

---

† The geometric distance is based on X-ray crystallographic studies of the related chromophore, $(NC)_5Fe^{II}-CN-Ru^{III}(NH_3)_5py^{1-}$, where py is pyridine.
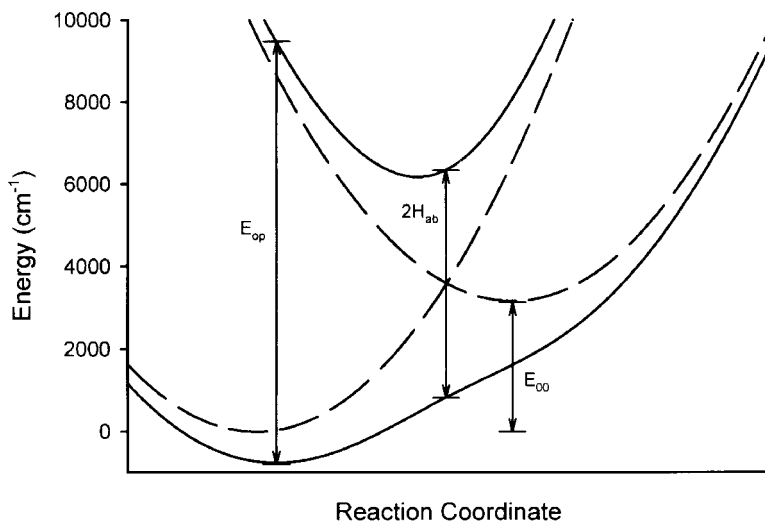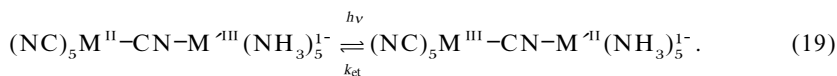
Figure 3.   Potential energy surfaces shown for $(CN)_5Fe-CN-Ru(NH_3)_5^{1-}$. Dashed line: diabatic surfaces. Solid line: adiabatic surfaces.

Figure 3 illustrates, for the related chromophore, $(NC)_5Fe-CN-Ru(NH_3)_5^{1-}$, the striking effects of electronic perturbations upon the two-dimensional surfaces for intervalence charge transfer. In the figure, the adiabatic reaction surfaces have been constructed from diabatic surfaces by utilizing H_{ab} in a simple first-order perturbation theory treatment.

3.8. $(NC)_5M^{II}-CN-M'^{III}(NH_3)_5^{1-}$: electron transfer implications

In order to understand better the intervalence charge transfer (IVCT) that occurs in compounds such as those presented in section 3.7, the related chromosphores $(NC)_5M^{II}-CN-M'^{III}(NH_3)_5^{1-}$ where $M^{II} = Fe^{II}$, Ru^{II}, and Os^{II} and $M'^{III} = Ru^{III}$ and Os^{III} have also been studied via Stark spectroscopy [14, 48]. As expected, the electroabsorption spectra are largely second derivative in nature, consistent with the charge transfer nature of these chromophores (i.e. large $\Delta\mu$):

$$(NC)_5M^{II}-CN-M'^{III}(NH_3)_5^{1-} \underset{k_{et}}{\overset{h\nu}{\rightleftharpoons}} (NC)_5M^{III}-CN-M'^{II}(NH_3)_5^{1-}. \tag{19}$$

$$M = Fe, Ru \text{ or } Os$$
$$M' = Ru \text{ or } Os$$

Surprisingly, the charge transfer distance, R_{12}, was found to vary little with metal substitution, ranging only from 2.4 to 3.8 Å for the entire family of chromophores. Thus it seems that the constant factors present, such as the ligand field effects and electron counts, have a larger influence on R_{12} than effects like the electronegativity and formal potential of the metal centre.

One particularly interesting finding within this family is the role Os^{II} plays as an electron donor. The nominally orthogonal transition from the d_{xy} orbital on the donor metal becomes allowed due to spin–orbit coupling. (The z axis is defined as the metal–metal axis.) As a result, the absorption spectra show an additional IVCT band at higher energy and of lower intensity than the usual transition originating from a d_{xz} or d_{yz} donor orbital. Since the two bands are not well resolved, even at the low

temperatures employed, this can lead to a non-unique fit of the Stark spectra. However, what is apparent from the data is that two bands are perturbed in a different manner by the electric field, as a fit obtained by assuming only a single electronic transition was unable to reproduce the electroabsorption lineshape.

Although $\Delta\mu$ shows no systematic dependence on the identity of the metal centres employed, the change in polarizability as measured by $\mathrm{Tr}\,(\Delta\alpha)$ is highly dependent on the identities of both the metal donor and metal acceptor. Using equation $(7c)$ to evaluate the B_x coefficients reveals that $\mathrm{Tr}\,(\Delta\alpha)$ ranges between -10 and $+560\ \mathrm{\AA}^3$. Interestingly, there is a good qualitative inverse correlation between these measured values and the energies of the IVCT bands. This can be at least partially understood by application of a two-level, two-state model for polarizability, given in equation (20) [7]:

$$\Delta\alpha_{12} = \alpha_2 - \alpha_1 = -2\alpha_1 = -4\frac{\mu_{12}^2}{E_{\mathrm{op}}}. \tag{20}$$

When the experimental values of $\mathrm{Tr}\,(\Delta\alpha)$ are plotted against the right hand side of equation (2), a correlation is displayed, but: (1) the magnitude of the values and resulting slope are *ca.* two orders of magnitude larger than equation (20) predicts, and (2) there is a large positive intercept which depends strongly on the identity of the acceptor metal. From these shortcomings, it is apparent that an accurate description of the polarizability changes accompanying intervalence excitation of these molecules requires an alternative or more complex theory. Presumably, such a theory would include a summation over the available excited states, rather than the singular state considered here. If so, experimental $\Delta\alpha$ values may provide a particularly sensitive diagnostic for upper excited state participation in nominally 'simple' intervalence charge transfer processes.

3.9. $(NC)_5 M^{II}-CN-M'^{III} (NH_3)_5^{1-}$: nonlinear optics implications

One interesting application of electroabsorption spectroscopy is the prediction or interpretation of certain nonlinear optical (NLO) responses. Within a two-level description, the second order NLO behaviour, responsible for frequency doubling of light, can be viewed as a virtual charge transfer process [49]. The molecular hyperpolarizability, β, is directly proportional to the quantity $\Delta\mu$, as shown in equation (21) [50]:

$$\beta = \frac{6\mu_{12}\,\Delta\mu_{12}\,E_{\mathrm{op}}^2}{[E_{\mathrm{op}}^2 - (2E_{\mathrm{inc}})^2][E_{\mathrm{op}}^2 - E_{\mathrm{inc}}^2]}. \tag{21}$$

In equation (21), E_{op} is the energy of the absorption maximum, E_{inc} is the energy of incident radiation, and the numeric subscripts indicate that a two level system is explicitly assumed. The transition moment, μ_{12}, can be found directly from the absorption experiment by applying equation (11). (Note that μ_{12} is equivalent to the quantity designated as **m** in other contexts.) Thus, the only ambiguity remaining is the sign of $\Delta\mu$, since the Stark experiment yields only the absolute value. In practice, the sign can often be inferred from chemical and structural considerations.

Molecules possessing intervalence charge transfer transitions should be reasonable candidates for NLO materials applications, since these transitions are often charac- terized by considerable charge transfer character and fairly low energy maxima (see equation (21)). A recent article by Laidlaw *et al.* [51] reported a β value of $\sim 200 \times 10^{-30}$ esu for $(NC)_5 Ru^{II}-CN-Ru^{III}(NH_3)_5^{1-}$ based on 1064 nm excitation.

From equation (21), based on a $\Delta\mu$ value of $-2.8\ e\mathrm{\AA}$ $(-13.4\ \mathrm{D})$ for

$(NC)_5 Ru^{II}-CN-Ru^{III}(NH_3)_5^{1-}$, the predicted β at 1064 nm is 40×10^{-30} esu [48]. This is smaller by a factor of five than the experimentally determined value, and is suggestive of one of the shortcomings of application of the two-level model to real systems. Since the simplified model includes no damping effects, it essentially assumes an infinitely narrow transition. Since the width of the IVCT absorption is ~ 4000 cm^{-1}, the assumption is a poor one. Furthermore, since the experimental bandwidth clearly has its origin primarily in vibrational Franck–Condon effects, standard damping models based on lifetime-induced dephasing are unlikely to capture correctly the effects of lineshape broadening upon frequency-dependent NLO responses. Since the transition is nearly resonant in both a one and two photon sense (i.e. both terms in the denominator of equation (21) are small but finite) the addition of appropriate damping or broadening terms would almost certainly bring the two-level model into closer agreement with theory.

Even in the absence of appropriate damping terms, the two-level model can be used to make some important qualitative predictions. Evaluation of equation (21) for the full set of systems discussed in section 3.8 reveals a trend in calculated β values that is dominated by variations in the IVCT transition energy. As such, it predicts that the largest zero-frequency NLO response will be generated by $(NC)_5 Fe^{II}-CN-Ru^{III}(NH_3)_5^{1-}$, i.e. the chromophore featuring the lowest lying IVCT transition. Of course, at other excitation energies, other chromophores could show larger responses due to resonance effects [48].

3.10. $(NC)_5 M^{II}-CN-Ru^{III}(NH_3)_4 pyridine^{-1}$: axial ligand effects

One interesting extension to the IVCT electroabsorption studies discussed in the last three sections is an investigation of the effects of axial ligand substitution. For example, if the ammonia ligand *trans* to the bridging CN is replaced by pyridine, as in the compounds $(NC)_5 M^{II}-CN-Ru^{III}(NH_3)_4 py^{-1}$ where $M^{II} = Fe^{II}$ or Ru^{II}, the Stark-determined charge transfer distance is increased by almost 1 Å [47].

$$(22)$$
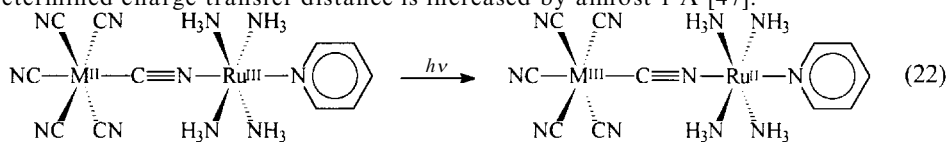
This is probably an indication that in the excited state, the acceptor Ru ion is able to donate electron density into the pyridine ligand through π back-bonding (an effect not achievable with a *trans* ammonia ligand). Regardless of the explanation, the extension in charge-transfer distance, together with the diminished absorption energy maximum, leads via the two level model to a predicted zero-frequency hyperpolarizability for $(NC)_5 Fe^{II}-CN-Ru^{III}(NH_3)_4 py^{1-}$ that is nearly ten times that estimated for $(NC)_5 Ru^{II}-CN-Ru^{III}(NH_3)_5^{1-}$, making the *trans* derivatized chromophore an attractive candidate for future NLO studies.

3.11. *Porphyrin based push–pull chromophores*

The first electroabsorption spectrum of a porphyrin was reported by Davidsson, who examined both the Q and the Soret bands of free base and iron (III) chloride-tetraphenylporphrin [52]. He used the technique to uncover several weak bands in the absorption spectrum of the Fe-containing molecule. In addition, for the free base molecule he observed, for several bands, unexpected (albeit small) dipole moment

changes. Nevertheless, the overall electroabsorption lineshape was dominated by the expected polarizability effects.

More recently, a study by Karki *et al.* [53] has made use of electroabsorption data to understand better the large first hyperpolarizabilities of selected donor–acceptor modified porphyrin systems. The compound [5-[[4′-(dimethylamino)phenyl]ethynyl]-15[4″-nitrophenyl)ethynyl]-10,20-diphenylporphinato]zinc(II), had previously been studied by hyper-Rayleigh scattering (HRS).
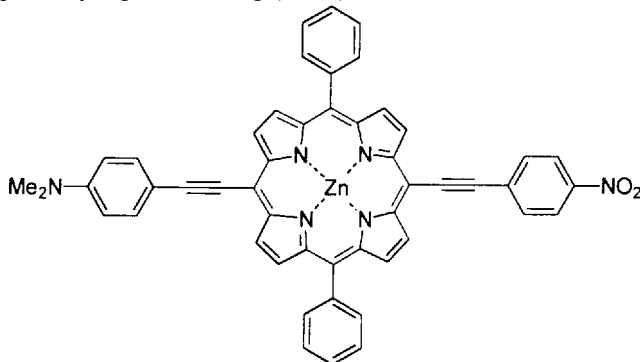
It displayed a $|\beta|$ of *ca.* 5000×10^{-30} esu which remained unchanged when the wavelength of incident light was changed from 830 to 1064 nm [54]. Interestingly, ZINDO based calculations, while highlighting the importance of charge transfer transitions, were unable to account for the wavelength independence of β, and underestimated its value by nearly an order of magnitude [55].

By experimentally examining the seven observable electronic and vibronic transitions in the Q and B (Soret) band regions, Karki *et al.* were able to determine the $|\Delta\mu|$ values for each transition and then predict the overall frequency-dependent hyperpolarizability of the chromophore via a summation of two-level contributions (equation (21)). Among the detailed findings were the following: (1) the calculated β values of 1700 and -1200×10^{-30} esu for incident radiation of 1064 and 830 nm, respectively, were in fair to good agreement with HRS derived values. (2) The experimentally determined $|\Delta\mu|$ values (and resulting β contributions) for the Q band transitions were larger than predicted by ZINDO calculations. (3) The near resonance conditions of the HRS experiment, at both wavelengths, were identified as key factors in creating the exceptionally large NLO responses.

3.12. *An NLO-active chromophore with an apparent octupolar architecture: Ru(4,4′-diethylaminostyryl-2,2′-bipyridine)$_3^{2+}$*

Octupolar chromophores provide an intriguing target for potential NLO applications [56]. The potential for noncentrosymmetric packing in a crystal lattice, a prerequisite for a bulk second order response, makes them particularly attractive for device applications. Studies with targets ranging from simple organic chromophores [57] to bacteriorhodopsin trimers in purple membranes [58] have shown that the octupolar symmetry provides a viable mechanism for frequency doubling. However, when the octupolar architecture is based around a metal centre, the symmetry of the ground and excited electronic states is less clear. Zyss *et al.* have shown that Ru(bpy)$_3^{2+}$ (bpy = 2,2′-bipyridine) is capable of producing light which is frequency doubled relative to the incident light [59], but there is a contention in the literature that two

photon absorption followed by luminescence obscures the measurement [60]. More recently, Dhenaut *et al*. have demonstrated the remarkable hyperpolarizability of $|\beta|$ = 2200×10^{-30} esu (1320 nm incident radiation) for the compound Ru(4,4′-dibutyl-aminostyryl-2,2′-bipyridine)$_3^{2+}$ [61], which does not appear marred by luminescence interference.

In work on a close structural analogue, Ru(4,4′-diethylaminostyryl-2,2′-bipyr-idine)$_3^{2+}$ (see drawing),
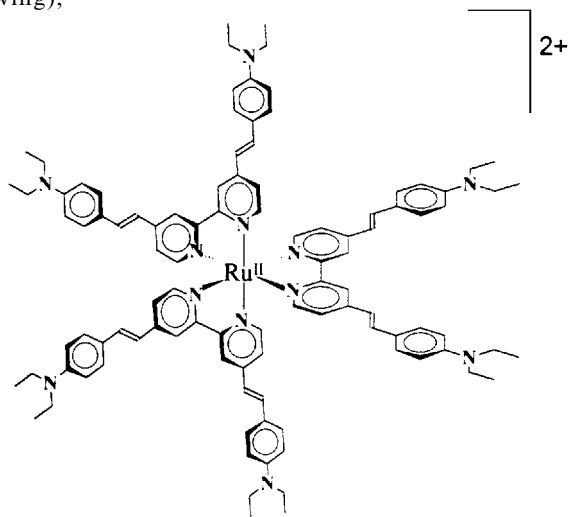
Vance *et al*. have probed the symmetry associated with the charge transfer transitions of the molecule [62]. Electroabsorption spectroscopy reveals that both the ligand-centred transition and the metal-to-ligand charge transfer transitions are highly Stark active, and that the activity is largely second derivative in nature. This indicates that in both instances a net displacement of charge occurs. This in turn indicates that the photo-excited electron is localized on one of the ligands, rather than delocalized over all three. Similar results indicating a localized excited state from electroabsorption spectroscopy have been reported by Oh *et al*. for Ru(bpy)$_3^{2+}$ (section 3.4) and by our lab for Ru(phenanthroline)$_3^{2+}$ (section 3.5). Additional evidence for excited state charge localization comes from polarized hyper-Rayleigh measurements which show that, despite the ground state structure, the symmetry of the transitions involved in frequency doubling are not octupolar, but rather have symmetry described by dominant charge transfer in one direction (i.e. excited state dipole-like behaviour).

4. Conclusions

Stark spectroscopy has proven to be a powerful tool for examining many of the intricacies associated with charge transfer in molecular compounds. For inorganic systems, the most extensive work has involved examination of MLCT and LMCT transitions occurring in mononuclear ruthenium complexes, where dipole moment contributions to the electroabsorption spectrum have been used to examine issues related to the effective charge transfer distance. Both ground state delocalization and the cumulative effects of many electrons interacting (i.e. not just the single electron nominally transferred) have proven to be important points. Electroabsorption spectra of metal-to-ligand charge transfer transitions in tris(diimine) compounds have provided additional evidence that charge is initially transferred to a single ligand

rather than to all three. Although quantitative interpretations of these spectra are still plagued by the badly overlapping transitions present in these systems, eventual examination of electro-emission spectra could alleviate these problems. Intervalence charge transfers in a range of bridged dinuclear systems have also been explored. Work on the pyrazine-bridged Creutz–Taube ion and the corresponding 4,4´-bipyridine-bridged ion has reinforced the delocalized description of the former, and shown that a naive 'geometric' interpretation of the charge transfer distance within the latter may lead to considerable error in the determination of related parameters such as the electronic coupling term and rate of thermal electron transfer. Extension of this work to CN bridged Fe, Ru, and Os complexes has uncovered interesting dependencies on both the metal centre and the ligand *trans* to the bridge. Electroabsorption data have also been used to make quantitative predictions about the nonlinear optical responses of these chromophores, and have been useful in delineating mechanisms of frequency doubling by others. Other interesting molecules which would be difficult to study with more traditional spectroscopies, such as the strongly delocalized dimacrocycles of Spreer and co-workers, have also been explored. Finally, the electroabsorption of inorganic systems is moving beyond its roots in simple, bridged metal compounds, with their unusual NLO and charge-transfer properties; studies of large porphyrinic and octupolar-like assemblies are suggestive of future directions.

Acknowledgements

References

[1] For example, ATKINS, P. W., 1994, *Physical Chemistry* (New York: W. H. Freeman and Company), Chap. 16.

[2] (*a*) JOHNSON, L. W., 1983, *J. chem. Phys.*, **79**, 1096; (*b*) HØG, J. H., BALLHAUSEN, C. J., and SOLOMON, E. I., 1976, *Molec. Phys.*, **32**, 807; (*c*) SOLOMON, E. I., BALLHAUSEN, C. J., and HØG, J. H., 1975, *Chem. Phys. Lett.*, **34**, 222.

[3] (*a*) MATHIES, R., and STRYER, L., 1976, *Proc. Natl. Acad. Sci. USA*, **73**, 2169; (*b*) MATHIES, R. A., 1974, PhD Dissertation, Cornell University, USA.

[4] (*a*) OH, D. H., SANO, M., and BOXER, S. G., 1991, *J. Am. chem. Soc.*, **113**, 6880; (*b*) OH, D. H., and BOXER, S. G., 1990, *J. Am. chem. Soc.*, **112**, 8161; (*c*) OH, D. H., 1991, PhD Dissertation, Stanford University, USA.

[5] OH, D. H., and BOXER, S. G., 1989, *J. Am. chem. Soc.*, **111**, 1130.

[6] (*a*) BUBLITZ, G. U., ORTIZ, R., MARDER, S. R., and BOXER, S. G., 1997, *J. Am. chem. Soc.*, **119**, 3365; (*b*) BUBLITZ, G. U., ORTIZ, R., RUNSER, C., FORT, A., BARZOUKAS, M., MARDER, S. R., and BOXER, S. G., 1997, *J. Am. chem. Soc.*, **119**, 2311.

[7] SHIN, Y. K., BRUNSCHWIG, B. S., CREUTZ, C., and SUTIN, N., 1996, *J. phys. Chem.*, **100**, 8157.

[8] (*a*) BOXER, S. G., 1996, *Biophysical Techniques in Photosynthesis*, edited by J. Amesz and A. J. Hoff (Netherlands: Kluwer), p. 177; (*b*) BOXER, S. G., 1993, *The Photosynthetic Reaction Center*, Vol. II, edited by J. Deisenhofer and J. R. Norris (San Diego: Academic Press), p. 179.

[9] BUBLITZ, G. U., and BOXER, S. G., 1997, *Ann. Rev. Phys. Chem.*, **48**, 213.

[10] (*a*) LIPTAY, W., 1974, *Excited States*, Vol. 1, edited by E. C. Lim (New York: Academic Press), p. 129; (*b*) LIPTAY, W., WALZ, G., BAUMANN, W., SCHLOSSER, H.-J., DECKERS, H., and DETZER, N., 1971, *Naturforsch*, **26a**, 2020; (*c*) LIPTAY., W., 1965, *Modern Quantum Chemistry*, Vol. 3, edited by O. Sinanoglu (New York: Academic Press), p. 45; (*d*) LIPTAY, W., 1969, *Angew. Chem. Int. Ed. Eng.*, **8**, 177; (*e*) Liptay, W., 1976, *Ber. Bunsenges*, **80**, 207.

[11] (*a*) VARMA, C. A. G. O., 1978, *Helv. Chim. Acta*, **61**, 772; (*b*) LIN, S. H., 1975, *J. chem. Phys.*, **62**, 4500.

[12] (*a*) REIMERS, J. R., and HUSH, N. S., 1991, *J. phys. Chem.*, **95**, 9773; (*b*) REIMERS, J. R., AND HUSH, N. S., 1991, *Mixed-Valency Systems: Applications in Chemistry, Physics, and Biology,* edited by K. Prassides (Dordrecht: Kluwer), p. 29.

[13] BOTTCHER, C. J. F., 1973, *Theory of Electric Polarization*, 2nd Edn., Vol. 1 (Amsterdam: Elsevier), pp. 74–86.

[14] KARKI, L., and HUPP, J. T., 1997, *J. Am. chem. Soc.*, **119**, 4070.

[15] (*a*) TAUBE, H., 1979, *Pure appl. Chem.*, **51**, 901; (*b*) FORD, P., RUDD, D. F. P., GAUNDER, R., AND TAUBE, H., 1968, *J. Am. chem. Soc.*, **90**, 1187.

[16] (*a*) ZWICKEL, A. M., and CREUTZ, C., 1971, *Inorg. Chem.*, **10**, 2395; (*b*) MAGNUSSON, R. H., AND TAUBE, H., 1975, *J. Am. chem. Soc.*, **97**, 5129.

[17] SHIN, Y. K., BRUNSCHWIG, B. S., CREUTZ, C., and SUTIN, N., 1995, *J. Am. chem. Soc.*, **117**, 8668.

[18] ZENG, J., HUSH, N. S., and REIMERS, J. R., 1996, *J. phys. Chem.*, **100**, 19292.

[19] CAVE, R. J., and NEWTON, M. D., 1996, *Chem. Phys. Lett.*, **249**, 15.

[20] CREUTZ, C., NEWTON, M. D., and SUTIN, N., 1994, *J. Photochem. Photobiol.* A: *Chem.*, **82**, 47.

[21] (*a*) MULLIKEN, R. S., 1952, *J. Am. chem. Soc.*, **74**, 811; (*b*) MULLIKEN, R. S., AND PERSON, W. B., 1969, *Molecular Complexes* (New York: Wiley).

[22] (*a*) HUSH, N. S., 1967, *Prog. Inorg. Chem.*, **8**, 391; (*b*) HUSH, N. S., 1968, *Electrochim. Acta*, **13**, 1005.

[23] CREUTZ, C., 1983, *Prog. Inorg. Chem.*, **30**, 1.

[24] TOM, G. M., CREUTZ, C., and TAUBE, H., 1974, *J. Am. Chem. Soc.*, **96**, 7827.

[25] HUPP, J. T., DONG, Y., BLACKBOURN, R. L., and LU, H., 1993, *J. phys. Chem.*, **97**, 3278.

[26] The two-sphere model: MARCUS, R. A., 1965, *J. chem. Phys.*, **43**, 679. Ellipsoidal cavity model: BRUNSCHWIG, B. S., EHRENSON, S., and SUTIN, N., 1986, *J. phys. Chem.*, **90**, 3657.

[27] See, for example, HUSH, N. S., 1985, *Coord. Chem. Rev.*, **64**, 135.

[28] (*a*) CREUTZ, C., and TAUBE, H., 1969, *J. Am. chem. Soc.*, **91**, 3988; (*b*) CREUTZ, C., and TAUBE, H., 1973, *J. Am. chem. Soc.*, **95**, 1086.

[29] (*a*) WONG, K. Y., and SCHATZ, P. N., 1981, *Prog. Inorg. Chem.*, **28**, 369; (*b*) PIEPHO, S. B., KRAUSZ, E. R., and SCHATZ, P. N., 1978, *J. Am. chem. Soc.*, **100**, 2996.

[30] (*a*) Ferreti, A., Lami, A., Ondrechen, M. J., and VILLANI, G., 1995, *J. phys. Chem.*, **99**, 10484; (*b*) ONDRECHEN, M. J., KO, J., and ZHANG, L.-T., 1987, *J. Am. chem. Soc.*, **109**, 1672; (*c*) ONDRECHEN, M. J., KO, J., and ZHANG, L.-T., 1987, *J. Am. chem. Soc.*, **109**, 1666; (*d*) KO, J., and ONDRECHEN, M. J., 1985, *J. Am. chem. Soc.*, **107**, 6161; (*e*) ONDRECHEN, M. J., KO, J., and ROOT, L. J., 1984, *J. phys. Chem.*, **88**, 5919.

[31] (*a*) PIEPHO, S. B., 1990, *J. Am. chem. Soc.*, **112**, 4197; (*b*) PIEPHO, S. B., 1988, *J. Am. chem. Soc.*, **110**, 6319.

[32] (*a*) LU, H., PETROV, A., and HUPP, J. T., 1995, *Chem. Phys. Lett.*, **235**, 521; (*b*) PETROV, V., HUPP, J. T., MOTTLEY, C., and MANN, L. C., 1994, *J. Am. chem. Soc.*, **116**, 2171.

[33] BEST, S. P., CLARK, R. J. H., MCQUEEN, R. C. S., and JOSS, S., 1989, *J. Am. chem. Soc.*, **111**, 548.

[34] (*a*) KRAUSZ, E., and MAU, A. W. H., 1986, *Inorg. Chem.*, **25**, 1484; (*b*) KRAUSZ, E., and LUDI, A., 1985, *Inorg. Chem.*, **24**, 939; (*c*) DUBICKI, L., FERGUSON, J., and KRAUSZ, E. R., 1985, *J. Am. chem. Soc.*, **107**, 179.

[35] For a recent review of intervalence charge transfer in ruthenium systems, see: Crutchley, R. J., 1994, *Adv. Inorg. Chem.*, **41**, 273.

[36] (*a*) SALAYMEH, F., BERHANE, S., YUSOF, R., DE LA ROSA, R., FUNG, E. Y., MATAMOROS, R., LAU, K. W., ZHENG, Q., KOBER, E. M., and CURTIS, J. C., 1993, *Inorg. Chem.*, **32**, 3895; (*b*) Chang, J. P., Fung, E. Y., and CURTIS, J. C., 1986, *Inorg. Chem.*, **25**, 4233.

[37] WILLIAMS, R. D., and HUPP, J. T., in preparation.

[38] For reviews of tris(diimine) complexes of ruthenium, see: (*a*) KALYANASUNDARAM , K., 1992, *Photochemistry of Polypyridine and Porphyrin Complexes* (New York: Academic Press), Chap. 6; (*b*) KRAUSZ, E., and FERGUSON , J., 1989, *Prog. Inorg. Chem.*, **37**, 293; (*c*) JURIS, A., BALZANI, V., BARIGELLETI, P., CAMPAGNA, S., BELSER, P., and VON ZELEWSKY, A., 1988, *Coord. Chem. Rev.*, **84**, 85; (*d*) MEYER, T. J., 1978, *Acc. Chem. Res.*, **11**, 94.

[39] (*a*) FORSTER , M., and HESTER , R. E., 1981, *Chem. Phys. Lett.*, **81**, 42; (*b*) Dallinger, R. F., and WOODRUFF , W. H., 1979, *J. Am. chem. Soc.*, **101**, 4391; (*c*) BRADLEY , P. G., KRESS, N., HORNBERGER , B. A., DALLINGER , R. F., and WOODRUFF , W. H., 1981, *J. Am. chem. Soc.*, **103**, 7441.

[40] See, for example, KOBER , E., SULLIVAN , B. P., and MEYER, T. J., 1984, *Inorg. Chem.*, **23**, 2098.

[41] HUG, S. J., and BOXER, S. G., 1996, *Inorg. Chem. Acta.*, **242**, 323.

[42] TURRO, C., YOUNG , Y. C., LEVANTIS , N., KUCHENMEISTER , M. E., WAGNER , P. J., and LEROI, G. E., 1996, *Inorg. Chem.*, **35**, 5104.

[43] KARKI, L., and HUPP, J. T., 1997, *Inorg. Chem.*, **36**, 3318.

[44] (*a*) ZHOU, J., LI, A., LANGE, C., ALLAN, C. B., SPREER, L. O., OTVOS, J. W., and CALVIN, M., 1996, *Inorg. Chem. Acta.*, **246**, 241; (*b*) MOUNTFORD , H. S., MACQUEEN, D. B., LI, A., OTVOS, J. W., CALVIN , M., FRANKEL , R. B., and SPREER, L. O., 1994, *Inorg. Chem.*, **33**, 1748; (*c*) SPREER , L. O., LI, A., MACQUEEN, D. B., ALLAN, C. B., OTVOS, J. W., CALVIN, M., FRANKEL , R. B., and PAPAEFTHYMIOU , G. C., 1994, *Inorg. Chem.*, **33**, 1753; (*d*) SPREER , L. O., ALLAN , C. B., MACQUEEN, D. B., OTVOS, J. W., and CALVIN, M., 1994, *J. Am. chem. Soc.*, **116**, 2187; (*e*) MOUNTFORD , H. S., SPREER, L. O., OTVOS, J. W., CALVIN , M., BREWER , K. J., RICHTER , M., and SCOTT, B., 1992, *Inorg. Chem.*, **31**, 717.

[45] KARKI, L., WILLIAMS , R. D., HUPP, J. T., ALLAN, C. B., and SPREER, L. O., 1998, *Inorg. Chem.*, in the press.

[46] KARKI, L., LU, H. P., and HUPP, J. T., 1996, *J. phys. Chem.*, **100**, 15637.

[47] VANCE, F. W., SLONE, R. V., STERN, C. S., and HUPP, J. T., manuscript in preparation.

[48] VANCE, F. W., KARKI, L., REIGLE, J. K., HUPP, J. T., and RATNER , M. A., submitted.

[49] (*a*) OUDAR , J. L., 1977, *J. chem. Phys.*, **67**, 446; (*b*) Oudar, J. L., and CHEMLA , D. S., 1977, *J. chem. Phys.*, **66**, 2664.

[50] WILLETS , A., RICE, J. E., BURLAND , D. M., and SHELTON , D. P., 1992, *J. chem. Phys.*, **97**, 7590.

[51] (*a*) LAIDLAW , W. M., DENNING , R. G., VERBEIST, T., CHAUCHARD , E., and PERSOONS, A., 1993, *Nature*, **363**, 58; (*b*) LAIDLAW , W. M., DENNING , R. G., VERBEIST , T., CHAUCHARD , E., and PERSOONS, A., 1994, *SPIE Proc.*, **2143**, 14.

[52] DAVIDSSON , A., 1980, *Chem. Phys.*, **45**, 409.

[53] KARKI, L., VANCE, F. W., HUPP, J. T., LECOURS, S. M., and THERIEN , M. J., 1998, *J. Am. chem. Soc.*, **120**, 2606.

[54] LECOURS, S. M., GUAN, H.-W., DIMAGNO, S. G., WANG, C. H., and THERIEN , M. J., 1996, *J. Am. chem. Soc.*, **118**, 1497.

[55] PRIYADARSHY , S., THERIEN , M. J., and BERATAN, D. N., 1996, *J. Am. chem. Soc.*, **118**, 1504.

[56] For a general review, see: ZYSS, J., and LEDOUX , I., 1994, *Chem. Rev.*, **94**, 77.

[57] (*a*) VERBEIST , T., CLAYS, K., SAMYN , C., WOLFF , J., REINHOUDT , D., and PERSOONS, A., 1994, *J. Am. chem. Soc.*, **116**, 9320; (*b*) KAATZ, P., and SHELTON , D. P., 1996, *J. chem. Phys.*, **105**, 3918.

[58] HENDRICKX , E., VINCKIER , A., CLAYS, K., and PERSSONS, A., 1996, *J. phys. Chem.*, **100**, 19672.

[59] ZYSS, J., DHENAUT , C., CHAUVAN , T., and LEDOUX, I., 1993, *Chem. Phys. Lett.*, **206**, 409.

[60] MORRISON , I. D., DENNING , R. G., LAIDLAW , W. M., and STAMMERS , M. A., 1996, *Rev. Sci. Instrum.*, **67**, 1445.

[61] DHENAUT , C., LEDOUX , I., SAMUEL , I. D. W., ZYSS, J., BOURGAULT , M., and LE BOZEC, H., 1995, *Nature*, **374**, 339.

[62] VANCE, F. W., SLONE, R. V., and HUPP, J. T., manuscript in preparation.